HHS Public Access

Author manuscript

Neuron. Author manuscript; available in PMC 2017 March 16.

Published in final edited form as:

Neuron. 2016 March 16; 89(6): 1194–1207. doi:10.1016/j.neuron.2016.02.011.

Cerebellar Transcriptome Profiles of *ATXN1* Transgenic Mice Reveal SCA1 Disease Progression and Protection Pathways

Melissa Ingram[#1,2], **Emily A. L. Wozniak**[#1,3], **Lisa Duvick**[1,4], **Rendong Yang**[5], **Paul Bergmann**[6], **Robert Carson**[1,4], **Brennon O'Callaghan**[1,4], **Huda Y. Zoghbi**[7], **Christine Henzler**[#5,#], and **Harry T. Orr**[1,4,#]

[1]Institute for Translational Neuroscience, Minnesota Supercomputing Institute, University of Minnesota, Minneapolis, MN 55455

[2]Department of Genetics, Cell Biology, and Development, Minnesota Supercomputing Institute, University of Minnesota, Minneapolis, MN 55455

[3]Department of Neuroscience, Minnesota Supercomputing Institute, University of Minnesota, Minneapolis, MN 55455

[4]Department of Laboratory Medicine and Pathology, Minnesota Supercomputing Institute, University of Minnesota, Minneapolis, MN 55455

[5]RISS Bioinformatics, Minnesota Supercomputing Institute, University of Minnesota, Minneapolis, MN 55455

[6]Foresight Logic, Inc., Shoreview, MN 55126

[7]Departments of Molecular and Human Genetics, Pediatrics, and Howard Hughes Medical Institute, Baylor College of Medicine, Jan and Dan Duncan Neurological Research Institute at Texas Children[1]s Hospital, Houston, TX 77030

[#] These authors contributed equally to this work.

SUMMARY

SCA1, a fatal neurodegenerative disorder, is caused by a CAG expansion encoding a polyglutamine stretch in the protein ATXN1. We used RNA sequencing to profile cerebellar gene expression in *Pcp2-ATXN1[82Q]* mice with ataxia and progressive pathology and *Pcp2-*

[#]Co-corresponding authors: C.H.; 612-625-0056, chenzler@umn.edu and H.T.O.; 612-625-3672, orrxx002@umn.edu. .

SUPPLEMENTAL INFORMATION

Supplemental information includes six figures and six tables, and can be found with this article online at http://

AUTHOR CONTRIBUTIONS

M.I., E.L. and H.T.O. contributed to the conception and design of the study. M.I., E.L., and L.D. contributed to tissue selection, collection and analyses. M.I., and E.L. performed RNA extractions for RNA- seq. M.I., E.L., C.H., R.Y. and P.B. performed RNA-seq expression and WGCNA bioinformatics analyses and carried out IPA analyses. C.H. supervised bioinformatics analyses. R.C. and B.O. performed *Atxn1*$^{2Q/154Q}$ qRT-PCR analyses. M.I., E.L. C.H. H.Y.Z. and H.T.O. interpreted the data and prepared the manuscript. All authors contributed to revision and intellectual content of manuscript and approved final version for publication.

ACCESSION CODES: RNA-seq data are deposited at NCBI Gene Expression Omnibus with the series accession GSE75778.

ATXN1[30Q]D776 animals having ataxia in absence of Purkinje cell progressive pathology. Weighted Gene Coexpression Network Analysis of the cerebellar expression data revealed two gene networks that significantly correlated with disease and have an expression profile correlating with disease progression *ATXN1[82Q]* Purkinje cells. The Magenta Module provides a signature of suppressed transcriptional programs reflecting disease progression in Purkinje cells, while the Lt Yellow Module, reflects transcriptional programs activated in response to disease in Purkinje cells as well as other cerebellar cell types. Furthermore, we found that upregulation of cholecystokinin *(Cck)* and subsequent interaction with the Cck1 receptor likely underlies the lack of progressive Purkinje cell pathology in *Pcp2-ATXN1[30Q]D776* mice.

INTRODUCTION

Functional genomics is increasingly being applied to the study of the CNS and neurodegenerative disease (Parikshak et al., 2015). Such studies provide inroads into defining the molecular settings of different regions and across different cell types within the CNS. Yet delineation of disease transcriptional signatures, i.e. elucidating which alterations in gene expression contribute to a disease process, remains a challenge. Distinguishing changes in expression that drive disease progression from those that are a result of disease, as well as identifying protective pathways whose activation mitigate disease, are critical for revealing potential therapeutic targets.

Among inherited neurodegenerative diseases are those caused by expansion of a CAG nucleotide repeat encoding a stretch of glutamines in the protein, the polyglutamine (polyQ) diseases. The polyQ neurodegenerative disease spinocerebellar ataxia type 1 (SCA1) is a lethal, progressive, autosomal dominant disorder caused by a CAG expansion in the Ataxin-1 (*ATXN1*) gene (Orr et al., 1993). SCA1 patients typically display loss of coordination of the limbs and trunk, unstable gait, dysarthria, and nystagmus (Klockgether, 2011). A prominent and consistent SCA1 pathological feature is the loss of cerebellar Purkinje cells (PCs) (Koeppen, 2005).

Several conserved sequence motifs in the ATXN1 protein, as well as cellular molecules that interact with ATXN1, indicate that ATXN1 functions in the nucleus as a regulator of transcription and RNA-processing. One such motif is the ATXN1/HBP1 (AXH) domain, residues 567-689 that folds into an OB-fold, forming putative RNA-binding and protein-protein interaction surfaces (Yue et al., 2001; de Chiara et al., 2003; Chen et al., 2004; Kim et al., 2013a). Several transcription regulators including SMRT (Tsai et al., 2004), Gfi-1 (Tsuda et al., 2005), Capicua (Lam et al., 2006; Kim et al., 2013a), and the Rora/Tip60 complex (Serra et al., 2006; Gehrking et al., 2011) interact with ATXN1 via its AXH domain. Importantly, polyQ expanded ATXN1 lacking the AXH domain is no longer pathogenic (Tsuda et al., 2005).

Towards the C-terminus from the AXH domain is another stretch of highly conserved overlapping sequence motifs in ATXN1. Among these are a nuclear localization signal (NLS) at amino acids 771-774 the function of which is required for pathogenesis (Klement et al., 1998), and a phosphorylation site at Ser 776 (S776) (Emamian et al. 2003; Huttlin et al., 2010). Placing a non-phosphorylatable Ala at position 776 renders ATXN1[82Q]

nonpathogenic (Emamian et al., 2003), likely by enhancing the clearance of ATXN1 (Jorgensen et al., 2009), and perhaps by decreasing the interaction of ATXN1 with RBM17 a splicing factor (Lim et al., 2008). While the extent to which an Asp at position 776 mimics phosphorylation is unclear (de Chiara et al., 2009), placing an Asp at this position enhances ATXN1/RBM17 interaction and PC pathogenesis of ATXN1[82Q], and transforms wild type ATXN1[30Q] into a pathogenic protein (Lim et al., 2008; Duvick et al., 2010). While mice expressing *ATXN1[30Q]-D776* manifest severe ataxia from an early age, i.e. as severe as *ATXN1[82Q]* animals, disease in *ATXN1[30Q]-D776* does not have progressive cerebellar pathology culminating with PC death as seen in *ATXN1[82Q]* mice.

Thus, these mouse models provide a means by which to identify pathways associated with a crucial aspect of SCA1, the progressive loss of PCs from the cerebellar cortex. To elucidate the role alterations in gene expression have in disease progression, we obtained longitudinal RNA sequence (RNA-seq) datasets on poly(A)$^+$ RNA from cerebella of *Pcp2-ATXN1[82Q]* and *Pcp2-ATXN1[30Q]-D776* mice at three ages representing early, moderate, and late stages of disease. Weighted Gene Coexpression Network Analysis revealed one PC-enriched gene module, the Magenta Module, for which an age-dependent down regulation of its eigengene associated with disease in *ATXN1[82Q]* mice. In addition, we found that expression of the cholecystokinin (*Cck*) gene was highly upregulated in *ATXN1[30Q]D776* cerebellar RNA. Moreover, loss of *Cck* function in *ATXN1[30Q]D776* mice enabled manifestation of progressive PC pathology, indicating that elevated *Cck* expression in *ATXN1[30Q]D776* mice is protective against progressive disease.

RESULTS

Overview of ATXN1 mouse lines and data production

To identify cellular pathways contributing to SCA1-like disease in the cerebellum of *ATXN1* transgenic mice, we used RNA-seq to profile expression. Mice utilized had *ATXN1* transgene expression directed specifically to PCs using an 850 bp portion of the 5′ upstream region from the *Pcp2/L7* gene (Vandaele et al., 1991; Burright et al., 1995). Transgenic lines used included previously described *ATXN1[82Q]* (line BO5, expressing *ATXN1* with a pure $(CAG)_{82}$ repeat tract) and *ATXN1[30Q]* (line AO2, expressing ATXN1 with an interrupted $(CAG)_{12}$-CAT-CAG-CAT-$(CAG)_{15}$ repeat tract) (Burright et al., 1995), along with *ATXN1[30Q]D776* (line 2) mice that express ATXN1 with a unexpanded human polyQ 30-repeat tract, $(CAG)_{12}$-CAT-CAG-CAT-$(CAG)_{15}$, and a potentially phospho-mimicking Asp residue at position 776 (Duvick et al., 2010). Like *ATXN1[82Q]* mice, *ATXN1[30Q]D776* animals develop severe ataxia from an early age. However, in contrast to the progressive Purkinje cell pathology displayed by *ATXN1[82Q]* mice, pathology in *ATXN1[30Q]D776* mice fails to progress beyond that typical of a mid-stage in *ATXN1[82Q]* animals. *ATXN1[30Q]D776* PC pathology does not advance to cell death.

RNA-seq was performed on cerebellar RNA isolated from *ATXN1* transgenic and wild type/FVB/NJ (wt) animals at 5, 12, and 28 weeks of age; ages corresponding to mild, moderate and severe ataxia, respectively, in *ATXN1[82Q]* mice but prior to onset of Purkinje cell death (Clark et al.,1997). In the case of *ATXN1[30Q]* mice, cerebellar RNA was isolated from five-week-old animals. Cerebellar RNA samples had RINs ranging from 7.9-9.3 with

an average RIN of 8.7 (Table S1). Using three biological replicates/genotype, a total of 1.5 billion paired-end reads were generated with a minimum of 27.5 million reads/genotype at each age. Following data quality control and prepping, the samples were mapped to the UCSC mm10 mouse annotated genome. Between 70-90% read pairs were correctly mapped, with most samples having a greater than 80% mapping efficiency.

Overview of cerebellar gene expression changes in *ATXN1* mice

As a first step in analysis of the ATXN1 mouse cerebellar RNA-seq data, we performed a principal component analysis (PCA) (Figure 1A). This analysis showed that data tended to cluster into three broad groups correlating with disease status. One large cluster included all samples from 5-week-old *ATXN1* transgenic animals (*ATXN1[30Q], ATXN1[30Q]D776*, and *ATXN1[82Q]* mice) and wt cerebellar samples at all ages, i.e. samples from all unaffected and mildly affected animals. A second cluster consisted of 12-week samples from moderately affected mice, *ATXN1[82Q]* and *ATXN1[30Q]D776*. The third cluster included samples from severely ataxic 28 week *ATXN1[82Q]* and *ATXN1[30Q]D776* mice. PCA analysis failed to distinguish changes in gene expression in *ATXN1[82Q]* mice having a disease with progressive pathology from *ATXN1[30Q]D776* animals where disease lacked progressive Purkinje cell pathology (Duvick et al., 2010).

We next evaluated RNA-seq data in pairwise comparisons using CuffDiff. Upon comparing *ATXN1[82Q]* and *ATXN1[30Q]D776* cerebellar gene expression data with wt at 5, 12 , and 28 weeks of age, similar to previous results (Crespo-Barreto et al., 2010; Lin et al., 2000; Serra et al., 2004), the majority of *ATXN1[82Q]* and *ATXN1[30Q]D776* significant differences were genes downregulated in comparison to wt (Figure S1A). This was particularly the case for the *ATXN1[82Q]* vs wt comparisons at 5 and 12 weeks of age. While the absolute number of significant changes in gene expression increased with age in *ATXN1[82Q]* vs wt mice, the peak absolute number of *ATXN1[30Q]D776* expression changes was found in 12 week old cerebella that decreased considerably in 28 week old *ATXN1[30Q]D776* samples.

To assess changes in expression within each genotype as mice aged, we compared expression changes within *ATXN1[82Q], ATXN1[30Q]D776*, and wt cerebella between 5 and 12, and 28 weeks of age (Figure S1B). Both *ATXN1[82Q]* and *ATXN1[30Q]D776* samples showed a greater number of genes whose expression changed across the three ages than was seen in wt samples. In *ATXN1[82Q]* mice between 5 and 12 weeks, the number of genes downregulated far out-numbered genes upregulated in expression. This pattern reversed between 12 and 28 weeks in *ATXN1[82Q]* mice, where an increase in the total number of genes with expression changes led to more genes being upregulated than downregulated. The pattern of gene expression change in *ATXN1[30Q]D776* mice between 5 and 12 weeks of age was very similar to that seen in *ATXN1[82Q]* mice both in terms of the number of genes whose expression changed and with downregulated genes out numbering upregulated genes. In contrast to the gene expression pattern In *ATXN1[82Q]* cerebella between 12 and 28 weeks, in *ATXN1[30Q]D776* mice the overall number of genes whose expression changed was decreased. This was largely due to a dramatic reduction in the number of genes with a downregulated pattern of expression between 12 and 28 weeks.

Thus, the overall similarity in the pattern of gene expression changes in the *ATXN1[82Q]* and *ATXN1[30Q]D776* mice in the 5-12 week age span is consistent with the finding that both ATXN1 mice develop severe ataxia and initial signs of Purkinje cell atrophy during this period. On the other hand, absence of a decrease in downregulated genes between 12 and 28 weeks in *ATXN1[30Q]D776* compared to *ATXN1[82Q]* cerebella correlates with an absence of a progressive PC pathology in *ATXN1[30Q]D776*.

SCA1 mouse cerebellum gene coexpression networks

To gain insight into cerebellar transcriptome organization from the *ATXN1* mice, we applied Weighted Gene Coexpression Network Analysis (WGCNA) to RNA-seq data from *ATXN1[82Q]*, *ATXN1[30Q]* and wt mice at 5, 12 , and 28 weeks (Zhang and Horvath, 2005; Langfelder and Horvath, 2008). This allowed identification of gene sets whose expression significantly correlated with one another across the three ages. Nineteen modules were detected with two, Magenta and Lt Yellow, being highly significantly associated with ataxia (t-test, adjusted p-values of 8e-09 and 1e-06, respectively) (Figure 1B and Tables S2 and S3).

As a means of identifying key genes and pathways in the two ataxia-associated WGCNA modules, we generated connectivity diagrams depicting genes with the highest connectivity (hubs) within each network. For the Magenta Module, all hub genes were down-regulated in *ATXN1[82]* and *ATXN1[30Q]D776* cerebella relative to wt. Of the ten most connected hub genes (Figure 2A), all are highly expressed by PCs with nine being expressed exclusively by PCs (Figure S2). Moreover, eight of the most connected hubs encode proteins involved in signal transduction (Table S4). In contrast, Lt Yellow network hub genes included down-regulated and up-regulated genes (*ATXN1[82Q]* and *ATXN1[30Q]D776* cerebella relative to wt) and included genes encoding proteins with a variety of functions (Figure 2B and below).

To further query the ataxia associated WGCNA gene Modules for biological meaning, Ingenuity Pathway Analysis (IPA) was performed. IPA of the Magenta Module revealed ATXN1 to be the most significant (p-value of 5.91e-08) upstream regulator of this module (Table S5), indicating that changes in Magenta Module gene expression are linked to ATXN1. IPA further showed that the most significant canonical pathways were all signaling pathways. The two most significant were synaptic long-term depression (p-value 1.49e-05) and glutamate receptor signaling (p-value 2.7e-04) (Table S2), both of which have previously been implicated in pathogenesis of SCA1 and other ataxias (Serra et al., 2004; Carlson et al., 2009; Schorge et al., 2010).

IPA of the ATXN1 mouse cerebellar Lt Yellow Module revealed canonical pathways and upstream regulators not previously implicated in SCA1 or other neurodegenerative diseases (Table S5). The most significant IPA pathway was the planar cell polarity (PCP) signaling pathway (p-value of 1.45e-04). PCP signaling is a noncanonical pathway in which some members of the Wnt family activate a β-catenin independent pathway well known for its role in the organization of cell sheets during development, particularly in *Drosophia*. However, it is becoming evident that PCP signaling also is a critical regulator of neural functions, including axonal guidance, dendrite maturation, stem cell development, and neuron survival (Tissir and Goffinet, 2013). The most significant (p-value of 1.123-04) upstream regulator of

the Lt Yellow Module identified by the IPA was the Jun-protooncogene-D transcription factor, JunD.

A detailed assessment of the coexpression pattern of RNAs across the two disease-associated mouse SCA1 WGCNA cerebellar modules was summarized with a single representative expression profile, the eigengene (Figure 3). Consistent with earlier work showing that ATXN1 with an expanded polyQ tract largely mediates down-regulation of genes (Lin et al., 2000), the Magenta eigengene was lower at all ages in the *ATXN1* transgenic lines that develop ataxia, *ATXN1[82Q]* and *ATXN1[30Q]D776*, compared to wt cerebella (Figure 3A). Intriguingly, while the Magenta eigengene remained constant with age in wt and *ATXN1[30Q]D776* cerebella, in *ATXN1[82Q]* cerebella the Magenta eigengene decreased substantially from 5 to 12 weeks of age and remained low in 28-week-old *ATXN1[82Q]* cerebella. Thus, the cerebellar Magenta Module eigengene correlated with a key phenotype difference between *ATXN1[82Q]* and *ATXN1[30Q]D776* mice - the progressive nature of disease in *ATXN1[82Q]* mice. Moreover, the failure of the Magenta eigengene to decrease with age in *ATXN1[30Q]D776* cerebellar RNA supports the conclusion that changes in gene expression within this module reflect a progressive disease phenotype.

In contrast to the Magenta Module, the Lt Yellow Module eigengene was somewhat higher in *ATXN1[82Q]* and *ATXN1[30Q]D776* cerebellar RNA compared to age matched wt samples (Figure 3B). Moreover, the Lt Yellow eigengene increased with age in *ATXN1[82Q]* cerebellar RNA and remained essentially constant in *ATXN1[30Q]D776* and wt samples. Thus, while the cerebellar Lt Yellow Module eigengene correlated with disease progression in *ATXN1[82Q]* mice, its change with age in *ATXN1[82Q]* increased rather than decreased as seen in the Magenta Module, suggesting that the underlying biology encoded by these two disease-associated modules differs.

Disease-associated coexpression modules differ in cerebellar cell type markers

Several lines of evidence indicate that the Magenta Module is enriched for genes preferentially expressed by PCs, while the Lt Yellow Module has a more substantial representation of genes expressed by multiple cerebellar cell types (Table 1). First, the Magenta Module showed highly significant overlap (p-value of 4.5e-16) with the cerebellar M6D WGCNA module identified from human brain microarray data (Oldham et al., 2007). Oldham et al. found that M6D is comprised largely of genes differentially expressed by PCs relative to other cerebellar cell types. Of the ten strongest members of M6D, four genes overlapped with the Magenta Module - including *Calb1* (the strongest member of M6D), *Itpr1*, *Plxdc1*, and *Pcp4*. In total, 19 genes overlapped between the human cerebellar M6D network and the mouse Magenta Module (Table 1). Of the 342 genes in the mouse ATXN1 cerebellar Magenta Module, 94 (Table 1) were among RNAs whose translation is enhanced in PCs (Doyle et al., 2008). The Lt Yellow Module, in contrast, had no genes that overlapped with the human cerebellar M6D Module and only one gene, lysophosphatidylglycerol acyltransferase 1 (Lpgat1), encoding RNA with enhanced PC translation (Table 1 and Table S3).

To assess the cerebellar cellular expression pattern of genes within the Magenta and Lt Yellow Modules, *in situ* hybridization (ISH) data from the Allen Brain Atlas was utilized (http://www.brain-map.org/; Len et al., 2007). This analysis revealed PC exclusive expression for 175 Magenta Module genes and 52 genes showing expression in multiple cerebellar cell types (Table 1 and Figure S2). To identify genes most strongly correlated with the eigengene expression in the most severely affected mice, we identified the 79 genes of the Magenta Module whose correlation with the eigengene for ATXN1[82Q] samples across all time points was 0.9 or greater. Of these genes, 61 (77%) had evidence of a PC-enriched pattern of expression and 16 were expressed by a wider range of cerebellar cell types. Of the 35 Lt Yellow Module genes, 11 genes showed PC exclusive expression by ISH, eight with PC enriched expression, and eight were equally expressed in multiple cell types. The number of genes in the Magenta Module whose expression was exclusive to PCs was 5.6-fold greater than the number of genes whose expression was distributed more uniformly among multiple cerebellar cell types (Table 1).

In contrast, analysis of the cerebellar cellular expression pattern of Lt Yellow module genes revealed that genes with a PC-exclusive pattern of expression was only1.4 fold greater than those expressed to a similar degree by other cerebellar cell types (Table 1 and Figure S3). Thus, compared to the Lt Yellow Module, the relative number of genes within the Magenta Module expressed specifically in PCs was considerably greater. Based on these data, we conclude that the Magenta Module is enriched for genes preferentially expressed by PCs while a greater proportion of Lt Yellow Module genes are expressed more widely by multiple cerebellar cell types.

The disease-associated WGCNA Magenta Module is enriched for genes regulated by ATXN1 interacting protein Cic

Among the ATXN1 protein interactors identified to date are several regulators of transcription including the Capicua homolog (Cic), SMRTER, GFI-1, and RORα/Tip60 (Tsai et al., 2003; Tsuda et al., 2005; Lam et al., 2006; Gehrking et al., 2011). To examine if genes of the Magenta and Lt Yellow Modules might be regulated by these ATXN1-interacting transcriptional factors, sequences 2.0kb upstream of the transcription start site of each gene in the Magenta and Lt Yellow Modules were extracted from the hg19 human genome reference and assessed for de novo motifs using MEME, DREME, and CentriMo (Machanic and Bailey, 2011). *De novo* motifs identified were compared with known motifs in the JASPAR and UniPROBE databases. RORα/Tip60 and Gfi-1 binding motifs were not significantly enriched in the upstream regions of Magenta or Lt Yellow genes. Cic and SMRT binding motifs were not in these databases. However, we were able to screen for two known Cic binding motifs, TGAATGAA and TGAATGGA (Kawamura-Saito et al., 2006). As a control each upstream sequence was randomly shuffled and screened for the binding motifs. The results showed that a highly significant number of Magenta Module genes have either one or both of the Cic binding motifs TGAATGAA and TGAATGGA in their upstream region with p values of 2.73e-12 and 5.85e-10, respectively (Table 2 and Table S6). Analysis of Lt Yellow Module genes revealed only the number of TGAATGGA motifs reached significance with a p value of 0.005 (Table 2). From these results we conclude that

the Magenta Module is enriched for genes whose expression is regulated by the ATXN1-interacting transcription factor Cic.

Magenta Module Purkinje cell-specific genes are down regulated in *Atxn1*$^{2Q/154Q}$ cerebella

The Magenta Module is unique in that it is enriched in genes preferentially expressed by PCs that seem to drive pathogenesis in *ATXN1[82Q]* mice. Thus, we were interested in examining whether Magenta gene expression is impacted similarly in a mouse model where mutant ataxin-1 is widely expressed from its endogenous regulatory elements. Towards accomplishing this, we used qRT-PCR to assess the expression of a set of Magenta genes in the cerebella of 12-week-old *Atxn1*$^{2Q/154Q}$ mice (Matilla et al., 1998). All the eight Magenta genes examined had module correlations of either greater than 0.9 or less than −0.9. Six of the genes were down-regulated in *ATXN1[82Q]* and *ATXN1[30Q]D776* cerebellar RNA compared to age matched wt samples (*Calb1*, *Itpr1*, *Inpp5a*, *Pcp4*, *Garnl3*, and *Rgs8*), with three of these being hubs (*Itpr1*, *Inpp5a*, and *Rgs8*). The other two genes examined were, Syt13 and Mxra7, both up-regulated in *ATXN1[82Q]* and *ATXN1[30Q]D776* cerebella. Figure S4 shows that all six of the genes down-regulated in *ATXN1[82Q]* and *ATXN1[30Q]D776* were significantly down in *Atxn1*$^{2Q/154Q}$ cerebellar RNA. In contrast, expression of neither of the two Magenta genes up-regulated in *ATXN1[82Q]* and *ATXN1[30Q]D776* changed in *Atxn1*$^{2Q/154Q}$ mice. This conservation in expression changes between *ATXN1[82Q]* and *ATXN1[30Q]D776* and *Atxn1*$^{2Q/154Q}$ mice provides further support for the concept that the down-regulated Magenta genes are critical for pathogenesis.

Elevated *Cck* activates a neuroprotective pathway in *ATXN1[30Q]-D776* cerebella mediated by Cck1 receptor

One potential explanation for the failure of PC pathology to progress in *ATXN1[30Q]D776* cerebella is that a neuroprotective pathway(s) was activated in these mice. If this were the case, we hypothesized that activation of a protective pathway might be reflected by elevated expression of critical genes in *ATXN1[30Q]D776* cerebellar RNA relative to wt and *ATXN1[82Q]* cerebellar RNA. We further reasoned that activation of a prominent pathway in *ATXN1[30Q]D776* cerebella might be reflected by a gene whose expression relative to wt is higher in *ATXN1[30Q]D776* and lower in *ATXN1[82Q]* mice. Of the 130 genes whose expression differed significantly between *ATXN1[30Q]D776* and *ATXN1[82Q]* as well as between each and wt (Figure 4A), 32 were upregulated in *ATXN1[30Q]D776* and downregulated in *ATXN1[82Q]* (Figure 4B). Of these 32, two, cholecystokinin (*Cck*) and collagen, type XVIII, alpha 1 (*Col18a1*), had expression levels of ≥ 3.0 FPKM and were previously identified as Purkinje cell markers (Rong et al., 2004; Doyle et al., 2008). Notably, *Cck* was expressed at far greater levels in *ATXN1[30Q]D776* compared to *ATXN1[82Q]* cerebella (Figure 4B). Furthermore, qRT-PCR confirmed that *Cck* expression relative to wt/FVB was significantly elevated in the cerebellum of all three lines of *ATXN1[30Q]D776* mice lacking progressive PC pathology, and decreased relative to wt in *ATXN1[82Q]* that have a progressive disease (Figure 4C).

To assess whether Cck has a role in cerebellar function/dysfunction, we first assessed *Cck*$^{-/-}$ mice (Lay et al.,1999) for altered cerebellar morphology and neurological status. By calbindin immunostaining, at 20 weeks and one year of age, PCs in *Cck*$^{-/-}$ mice were

indistinguishable from those in age-matched wt mice (Figure S5A). While *Cck*$^{-/-}$ mice showed no loss of PCs out to one year of age in *Cck*$^{-/-}$ cerebella (Figure S5B), there was a slight and significant decrease in thickness of the cerebellar molecular layer between 20 weeks and one year of age (Figure S5C). In addition, qRTPCR analysis revealed a significant reduction in expression of a PC marker *calbindin* (*Calb*) in cerebellar RNA from 1-year-old *Cck*$^{-/-}$ mice (Figure S5D). These analyses showed that while loss of *Cck* did adversely impact cerebellar morphology and function, it did not cause severe atrophy and loss of PCs.

We next assessed whether elevated Cck expression contributed to the lack of progressive PC disease in *ATXN1[30Q]D776* mice by crossing *Cck*$^{-/-}$ and *ATXN1[30Q]D776* mice. Examination of cerebellar pathology in one-year-old mice revealed more extensive PC pathology in *ATXN1[30Q]D776;Cck*$^{-/-}$ mice compared to one-year-old *ATXN1[30Q]D776* mice (Figure 5A). As measured by molecular layer thickness, *ATXN1[30Q]D776;Cck*$^{-/-}$ mice had a progressive atrophy of PC dendrites from 20 weeks to 1 year of age in contrast to *ATXN1[30Q]D776* mice that showed no progression in molecular layer atrophy between 20 weeks and one year of age (Figure 5B). Moreover, progression in molecular layer atrophy with age in *ATXN1[30Q]D776;Cck*$^{-/-}$ mice was essentially identical to that seen in *ATXN1[82Q]* cerebella. Absence of *Cck* in *ATXN1[30Q]D776* mice resulted in a progressive disease that included loss of PCs from the cerebellar cortex (Figure 5C). In addition, cerebella from *ATXN1[30Q]D776;Cck*$^{-/-}$ mice at 36 weeks of age displayed enhanced pathology compared to *ATXN1[30Q]D776* animals as assessed by atrophy of the molecular layer and loss of PCs (Figure 5D and 5E). Absence of *Cck* function in *ATXN1[30Q]D776* mice resulted in a more severe and progressive PC pathology similar to pathology in *ATXN1[82Q]* mice. These results are consistent with elevated *Cck* expression in *ATXN1[30Q]D776* mice affording protection against a form of PC pathology that progresses to cell death.

In the cerebellar cortex, *Cck* is predominately, if not exclusively, expressed by PCs (Rong et al., 2004; Doyle et al., 2008), a point further supported by ISH data from the Allen Brain Atlas (Figure S6). Cck, a prohormone, is processed to active peptides whose actions are mediated by two G-protein coupled receptors (Dufresne et al., 2006; Lee and Soltesz, 2011), Cck1R and Cck2R (first designated as Cckar and Cckbr). ISH data indicate that *Cck1r* is the one expressed in the adult mouse cerebellum in a PC-enriched manner (Figure S6). Given data presented here indicating that elevated *Cck* can protect PCs against disease progression to cell death coupled with the data that *Cck1r* is uniquely expressed in the mouse cerebellum by PCs, we speculated that the Cck protective effect in *ATXN1[30Q]D776* mice is via the Cck1r. To test this, we crossed *ATXN1[30Q]D776* mice with mice lacking either *Cck1R* or *Cck2R*. Consistent with the cerebellar cellular expression pattern of CckRs, *ATXN1[30Q]D776* mice lacking *Cck1R* developed a progressive PC pathology as assessed by atrophy of molecular layer thickness (Figure 6A and 6B) and loss of PCs with age (Figure 6C). In contrast, *ATXN1[30Q]D776/Cck2R*$^{-/-}$ mice showed the same lack of an age-dependent PC pathology as seen in *ATXN1[30Q]D776* animals (Figure 6) . Based on these data, we conclude that lack of a progressive PC pathology in *ATXN1[30Q]D776* mice is due

to the increased expression of Cck by *ATXN1[30Q]D776* PCs and cleavage of the proCck into a secreted peptide that activates PC Cck1Rs.

DISCUSSION

We performed an unbiased and comprehensive cerebellar gene coexpression analysis using a panel of transgenic mouse models in which *ATXN1* transgene expression was directed specifically to PCs, a prominent site of SCA1 pathology. Using cerebellar RNA-seq data obtained from mice with a disease that progressed from development of ataxia to death of PCs (*ATXN1[82Q]* mice) and from mice with a disease that failed to progress beyond development of ataxia (*ATXN1[30Q]D776* animals), we demonstrated that the cerebellar transcriptome in ATXN1 mice was organized into 19 modules or networks of coexpressed genes. Of these, the Magenta and Lt yellow modules, had expression patterns that significantly correlated with disease. Analyses of these two disease-associated gene coexpression networks supported a conclusion that the Magenta Module provides a signature of suppressed transcriptional programs reflecting disease progression in PCs, while the Lt Yellow Module reflects transcriptional programs activated in response to disease in PCs. Additional analyses of the RNA-seq data revealed that cerebella from mice with a non-progressive disease (*ATXN1[30Q]D776* mice) uniquely expressed elevated levels of RNA from the neuropeptide gene cholecystokinin (*Cck*). Deletion of *Cck* or *Cck1R* from *ATXN1[30Q]D776* animals converted disease from being non-progressive to one in which PC pathology progressed to cell death. These data reveal a Cck/Cck1R-mediated neuroprotective pathway(s) that might be exploitable as a therapeutic target.

While both the Magenta and Lt Yellow WGCNA modules were robustly associated with disease, features of these networks indicate they likely reflect distinct functions. Aspects of the Magenta Module support the concept that this module largely consists of changes in gene expression and pathways reflecting disease progression in PCs. First, a substantial proportion of the genes in the Magenta Module are genes with an elevated and often exclusive expression in PCs. Moreover, IPA of the Magenta Module revealed ATXN1 as the most significant upstream regulator of the Magenta Module. IPA also identified synaptic long term depression (LTD) and glutamate receptor signaling as top canonical pathways for the magenta module, both of which have previously been implicated in the pathogenesis of SCA1 as well as other ataxias (Serra et al., 2004; Schorge et al., 2010). Eigengene analysis of the Magenta Module revealed a modular expression showing a decreased pattern of expression relative to wt cerebellum at all ages with a dramatic decrease in expression as disease progressed from 5 to 12 weeks of age that remained low at 28 weeks of age. This is consistent with previous studies indicating that a major pathogenic effect of mutant ATXN1 is to cause a decrease in gene expression (Crespo-Barreto, et al., 2010).

Several studies support that interaction of expanded polyQ ATXN1 with the transcriptional repressor homolog of *Drosophila* Capicua (Cic) is a driver of cerebellar pathogenesis (Lam et al., 2006; Jafar-Nejad et al., 2011; Fryer et al., 2011). Thus, finding that genes within the Magenta Module are significantly enriched for Cic binding motifs within their upstream regions supports the concept that this gene network is enriched for genes whose alteration in expression directly reflect a pathogenic action of mutant ATXN1 that drives SCA1

progression in PCs. However, IPA of the Magenta genes that contain Cic-binding motifs indicated that these genes did not cluster within a single functional pathway per se (data not shown). The finding that all of a sub-set of Magenta genes down regulated in affected *ATXN1* transgenic mouse cerebella were also decreased in expression in *Atxn1*$^{2Q/154Q}$ cerebellar RNA indicates that down-regulation of genes in this module is common to PC disease across SCA1 mouse models, including one where mutant Ataxin-1 is widely expressed from the its endogenous locus.

Previous work highlighted that intramodular hubs, genes highly connected to other genes within a trait-associated network, often provide novel biological insight (Langfelder et al., 2013). Analysis of the Magenta Module revealed that all of its hubs corresponded to downregulated genes with a substantial proportion of the most highly connected hubs encoding components signaling pathways (Figure 2 and Table S4)). This suggests that with SCA1 disease progression PCs acquire considerable perturbations of intracellular signaling pathways. Of note, one of the top highly connected hub genes is a member of the family of potent negative regulators of G-coupled receptors, regulator of G-protein signaling 8 (Rgs8). *Rgs8*, was recently found to be downregulated in mouse models of SCA2 (Dansithing et al., 2015), indicating overlap in signaling alterations among the SCAs. Another magenta down-regulated hub gene having a Cic-binding site in its upstream region is Homer-3. Impairment of Homer-3 expression in *Atxn1*$^{2Q/154Q}$ PCs was recently shown to be a driver of pathophysiology (Ruegseggaer et al., 2016).

Compared to genes in the Magenta Module, the proportion of Lt Yellow Module genes with enhanced or exclusive expression in PCs was considerably less. In addition, the Lt Yellow Module has a much higher proportion of genes expressed by multiple cerebellar cell types. IPA of the Lt Yellow Module identified JunD as the most significant upstream regulator with no evidence of ATXN1 as an upstream regulator of this Module. While the biological significance of JunD as an upstream regulator is not readily apparent, it is worth noting evidence for JunD having a role in glutamate-induced excitotoxicity in cerebellar granule neurons (Lidwell and Griffiths, 2000). Likewise, IPA of the Lt Yellow Module identified PCP as its significant canonical pathway. While the PCP is typically viewed as a non-canonical Wnt signaling pathway with a critical role in the organization of cells and cell sheets during early embryonic development, the involvement of PCP genes in neuronal functions such as dendrite elaboration and neuron survival, are becoming increasingly apparent (Tissir and Goffinet, 2013; Liu et al., 2013). In support of the PCP having a role in cerebellar function is the identification of a mutation in human *PRICKLE1*, which encodes a core PCP protein, causing progressive myoclonus epilepsy-ataxia syndrome (Bassuk et al., 2008). Lastly, Lt Yellow genes were relatively devoid of Cic-binding motifs within their upstream regions. Thus, we suggest that the Lt Yellow Module reflects secondary affects of expressing mutant ATXN1 in Purkinje cells – perhaps compensatory pathways in PCs as well as other cerebellar cell types activated in response to disease.

Of the several WGCNA studies reported utilizing expression data from patients with neurodegenerative disease, two of note in relation to our work are a WGCNA using data from brain and peripheral tissues of patients with ataxia with oculomotor apraxia type 2 (AOA2) and an analysis of brain expression data, including data from the cerebellum, from

patients with C9orf72 associated and sporadic amyotrophic lateral sclerosis (ALS) (Fogel et al., 2014; Prudencio et al., 2015). AOA2 is due to recessive mutations in the Senataxin (*SETX*) gene while ALS4 is a juvenile form of ALS caused by dominant *SETX* mutations. The study by Fogel et al. identified two WGCNA modules specific to AOA2 and senataxin function, the Blue and Turquoise modules respectively. There was no significant overlap of either of our two SCA1 disease-associated modules with the Turquoise senataxin function AOA2 WGCNA Module. There were 42 genes of the SCA1 Magenta Module that overlapped significantly (p-value of 1.5e-3) with the Blue AOA2 transcriptional signature Module (Table S2). Ten of the genes that overlapped between the SCA1 Magenta Module and the AOA2 Blue Module had evidence of being PC markers, supporting the concept of an overlap in PC functional alteration in AOA2 and SCA1. Another study of potential relevance to our SCA1 WGCNA is one that used frontal cortex and cerebellar expression data from *C9orf72*-ALS affected brains (Prudencio et al., 2015). In this study, the most disease-significant cerebellar MEpink Module was enriched for genes encoding components of neuron development, protein localization and transcription pathways. Neither of the SCA1 disease-associated WGCNA modules showed overlap with the *C9orf72*-ALS MEPink WGCNA module, indicating that distinct cerebellar networks are affected in SCA1 and *C9orf72*-ALS.

ATXN1 mouse cerebellar RNA-seq analyses also revealed a substantial, unique and PC-specific upregulation of cholecystokinin *(Cck)* RNA in *Pcp2-ATXN1[30Q]D776* mice, in which PC disease is not progressive (Figure 4). Cck, originally discovered in the gastrointestinal tract, is one of the most abundant neuropeptides having selective effects on specific cell types and synapses (Lee and Soltesz, 2011). A consequence of enhanced expression of Cck in *ATXN1[30Q]D776* Purkinje cells in relation to their lack of progressive disease was disclosed by crossing *ATXN1[30Q]D776* mice with mice lacking either *Cck* or *Cck1R.* Absence of either Cck or Cck1R in *Pcp2-ATXN1[30Q]D776* mice resulted in a PC disease in which pathology now progressed to cell death. The natural ligand with the highest affinity for the Cck1R is Cck-8, an octapeptide cleaved from the C-terminal portion of Cck (Dufresne et al., 2006). Thus, these results strongly support a model where elevated Cck and its subsequent processing to a peptide that binds to Purkinje cell Cck1R in an autocrine manner underlies the lack of progressive Purkinje cell pathology in *ATXN1[30Q]D776* mice. A similar neuroprotective role for another neuropeptide NPY in mouse models of SCA3/MJD was recently reported by Duarte-Neves et al. 2015. Elucidation of a Cck/Cck1R pathway as being protective against a progressive SCA1-like PC disease has potential therapeutic implications. There are considerable *in vivo* data, including in humans, on the use of Cck1R agonists, peptides, peptoids, and small molecules, as satiety agents for the treatment of obesity disease (Asin et al., 1992; Cannon et al., 1996; Jordan et al., 2008; Wang et al., 2011). We suggest these data present a basis from which to examine Cck1R as a therapeutic target for preclinical modification of SCA1 cerebellar disease.

EXPERIMENTAL PROCEDURES

Mice

The Institutional Animal Care and Use Committee approved all animal use protocols. All mice were housed and managed by Research Animal Resources under SPF conditions in an AAALAC-approved facility. *Cck*$^{-/-}$, *Cck1R*$^{-/-}$ and *Cck2R*$^{-/-}$ mice were obtained from Jackson Labs, Bar Harbor, Me. (*Cck*$^{-/-}$; cat#017710/RRID: IMSR-JAX:017710, *Cck1R*$^{-/-}$; cat#006365/RRID:IMSR-JAX:006367 and *Cck2R*$^{-/-}$; cat#006365/RRID: IMSRJAX: 006369). In all experiments equal numbers of male and females were used.

RNA isolation and sequencing

Total RNA was isolated from dissected cerebella using TRIzol Reagent (Life Technologies, Carlsbad, California) following the manufacturer's protocols. Cerebella were homogenized using an RNase-Free Disposable Pellet Pestles in a motorized chuck. For RNA-sequencing, RNA was further purified to remove any organic carryover using the RNeasy Mini Kit (Qiagen, Venlo, Netherlands) following the manufacturer's RNA Cleanup protocol.

Cerebellar RNA from three biological replicates/genotype was isolated. Purified RNA was sent to the University of Minnesota Genomics Center for quality control, including quantification using fluorimetry (RiboGreen assay, Life Technologies) and RNA integrity assessed with capillary electrophoresis (Agilent BioAnalyzer 2100, Agilent Technologies, Inc.) generating an RNA integrity number (RIN). All submitted samples had greater than 1ug total mass and RINs 7.9 or greater (Table S1). Library creation was completed using oligo-dT purification of polyadenylated RNA, which was reverse transcribed to cDNA. cDNA was fragmented, blunt-ended, and ligated to barcoded adaptors. Library was size selected to 320bp +/− 5% to produce average inserts of approximately 200bp, and size distribution validated using capillary electrophoresis and quantified using fluorimetry (PicoGreen, Life Technologies) and q-PCR. Libraries were normalized, pooled and sequenced. 12 and 28 wk *ATXN1[82Q]*, *ATXN1[30Q]-D776*, and wt/FVB samples were sequenced on an Illumina GAIIX using a 76nt paired-end read strategy, while 5 wk samples from these genotypes were sequenced on an Illumina HiSeq 2000 using a 100nt paired-end read strategy. Data were stored and maintained on University of Minnesota Supercomputing Institute (MSI) Server.

Reads were aligned to mouse reference genome (mm10) with Tophat2 (Kim et al, 2013b) using mostly default parameters with two exceptions: mate inner distance and standard deviation were adjusted to the data and using a gene annotation model only looking for supplied junctions (mm10 gtf file from iGenomes). Reads were quantified using Cuffquant (Trapnell et al, 2010, Roberts et al, 2011), and differential gene expression was determined with Cuffdiff2 using default parameters (Trapnell et al, 2012). Genes/introns with a $q \leq 0.05$ were considered significant. Genome tracks were visualized with Integrated Genomics Viewer (Broad Institute). Results were graphed with CummeRbund (http://compbio.mit.edu/cummeRbund/; Goff et al., 2013). Pathway and clustering analysis was completed with Ingenuity Pathway Analysis (Ingenuity Systems, Redwood City, California). Normalized expression values of all genes across all samples were prepared from Cuffquant results using

Cuffnorm (Trapnell et al, 2010). The iGenomes mm10 gtf contains both miRNAs and snoRNAs, which are too small to be accurately sequenced using standard RNA-seq library preparation and sequencing. Including these short transcripts in the expression data used for the PCA resulted in PCs driven by the extreme expression of a few miRNAs and snoRNAs. Expression data used in the PCA was re-quantified using Cuffquant and Cuffnorm after removing miRNAs and snoRNAs from the iGenomes gtf.

Expression analyses

Gene expression analysis with the Tuxedo pipeline (Kim et al., 2013b; Trapnell et al., 2010). Initial read quality was assessed using FastQC (Andrews - Babraham Bioinformatics, FastO| QC A quality control tool for high throughput sequence data) and reads trimmed to remove low quality 3′ ends and adapter contamination using Trimmomatic (Bolger et al., 2014).

Reads were aligned to mouse reference genome mm10 with Tophat2 (Kim et al, 2013b) using mostly default parameters with two exceptions: mate inner distance and standard deviation were adjusted to the data and using a gene annotation model only looking for supplied junctions (mm10 gtf file from iGenomes). Reads were quantified using Cuffquant (Trapnell et al, 2010, Roberts et al, 2011), and differential gene expression was determined with Cuffdiff2 using default parameters (Trapnell et al, 2012). Genes/introns with a $q \leq 0.05$ were considered significant. Genome tracks were visualized with Integrated Genomics Viewer (Broad Institute). Results were graphed with CummeRbund (http://compbio.mit.edu/cummeRbund/; Goff et al., 2013). Pathway and clustering analysis was completed with Ingenuity Pathway Analysis (Ingenuity Systems, Redwood City, California: RRID:SCR-008653). Normalized expression values of all genes across all samples were prepared from Cuffquant results using Cuffnorm (Trapnell et al, 2010). The iGenomes mm10 gtf contains both miRNAs and snoRNAs, which are too small to be accurately sequenced using standard RNA-seq library preparation and sequencing. Including these short transcripts in the expression data used for the PCA resulted in PCs driven by the extreme expression of a few miRNAs and snoRNAs. As a result, the expression data used in the PCA was re-quantified using Cuffquant and Cuffnorm after removing miRNAs and snoRNAs from the iGenomes gtf.

WGCNA

FPKM abundance estimates for all 27 samples were produced by CuffNorm (Trapnell et al. 2012) and were $\log_2$ transformed ($\log_2$(FPKM+1)) for WGCNA analysis (Langfelder and Horvath, 2008). The WGCNA R package (v. 1.41) was used to construct an unsigned gene coexpression network with a soft threshold power [beta] of 10. Nineteen modules were detected, including two that were significantly associated with ataxia (wt vs *ATXN1[82Q]* and *ATXN1[30Q]D776* mice, t-test, Bonferroni corrected p-value < 1e-5). Data for Magenta and Lt Yellow modules was exported to Cytoscape for visualization. Network figures are limited to the top 20% of genes with the strongest network connections (the topological overlap threshold was raised until only 20% of genes remained). The network modules are color coded by the differential expression at week 12 as follows: green: significantly downregulated in B05 compared to FVB and in D30 compared to FVB; red: significantly upregulated in B05 compared to FVB and in D30 compared to FVB; gray: either not

significant in either or both of the two comparisons, or the direction is different between the two (e.g. up in B05 compared to FVB but down in D30 compared to FVB, or vice versa). The size of the circles is scaled by the absolute value of the mean log2 fold change between B05 and FVB, and between D30 and FVB.

To identify genes in the Magenta Module that were most correlated with the sickest mice, we identified the genes that had a correlation of 0.9 or greater with the Magenta Module eigengene values for the ATXN1[82Q] mice across all time points (9 data points).

To compare the genes in the Magenta and Lt Yellow modules to modules from other published WGCNA analyses, we followed the procedure of Oldham et al. (2008) to conduct a hypergeometric test for significant overlap.

Histology and immunostaining

Animals were anesthetized and transcardially exsanguinated with PBS (pH 7.4) and perfused using 10% formalin (30 mL). Brains were post-fixed overnight in 10% formalin and placed in PBS at 4°C before sectioning. Cerebella were sectioned into 50 m sagittal sections using a vibratome. Epitopes were exposed using antigen retrieval by boiling sections four times for 10 sec each in 0.01M urea. Sections were blocked overnight in 2% normal donkey serum and 0.3% Triton X-100 in PBS. Subsequent staining was carried out in 2% normal donkey serum and 0.3% Triton X-100 in PBS. Anti-calbindin antibodies used were (Sigmmouse a-Aldrich Cat# C9848/RRID:AB-10115846) and rabbit (Sigma-Aldrich Cat# C2724/RRID:AB-258818) at a 1:250 dilution.

Sections were incubated for 24 hrs with primary antibodies at 4°C. Following incubation, sections were washed three times in PBS and exposed to secondary antibodies (Alexa Fluor 488 antimuse-cat# 715-546/RRID:AB-2340850 and Alexa Fluor 647 antirabbit-cat# 711-605-152/RRID:AB-2492288}, Jackson Immunoresearch Labs, West Grove, PA) for 24 hrs at 4°C. Sections were washed three times in PBS and mounted onto charged slides (Colorfrost Plus, Fisher, Waltham, MA). Fluorescently labeled tissue was imaged using a confocal Olympus 1000 IX inverted microscope.

Supplementary Material

Refer to Web version on PubMed Central for supplementary material.

ACKNOWLEDGEMENTS

We thank Orion Rainwater for propagating and maintaining mouse colony; Dr. Jeehye Park and Ms. Antonia De Maio for their constructive comments. This study was supported by NIH/NINDS grant 2R37NS022920 (H.T.O.) and 2R37NS027699 (H.Y.Z).

REFERENCES

Asin KE, Bednarz L, Nikkel AL, Gore PA, Montana WE, Cullen MJ, Shiosaki K, Craig R, Nadzan AM. Behavioral effects of A71623, a highly selective CCK-A agonist tetrapeptide. Am. J. Physiol. 1992; 263:R125–R135. [PubMed: 1636779]

Bassuk AG, et al. A homozygous mutation in human PRICKLE1 causes an autosomal-recessive progressive myoclonus epilepsy-ataxia syndrome. Amer. J. Hum. Genet. 2008; 83:572–581. [PubMed: 18976727]

Bolger AM, Lohse M, Usadel B. Trimmomatic: A flexible trimmer for Illumina Sequence Data. Bioinformatics. 2014 btu170.

Burright EN, Clark HB, Servadio A, Matilla T, Feddersen RM, Yunis WS, Duvick LA, Zoghbi HY, Orr HT. SCA1 transgenic mice: a model for neurodegeneration caused by an expanded CAG trinucleotide repeat. Cell. 1995; 82:937–948. [PubMed: 7553854]

Cannon J, Adjei L, Lu M-Y, Garren K. Alternate drug delivery routes for A-71623, a potent cholecystokinin-a receptor agonist tetrapeptide. J. Drug Targeting. 1996; 4:69–78.

Carlson KM, Andresen MJ, Orr HT. Emerging pathogenic pathways in the spinocerebellar ataxias. Curr. Opin. Genet. Dev. 2009; 19:247–253. [PubMed: 19345087]

Chen YW, Allen MD, Veprintsev DB, Löwe J, Bycroft M. The Structure of the AXH Domain of Spinocerebellar Ataxin-1. J. Biol. Chem. 2004; 279:3758–3765. [PubMed: 14583607]

Clark HB, Burright EN, Yunis WS, Larson S, Wilcox C, Hartman B, Matilla A, Zoghbi HY, Orr HT. Purkinje cell expression of a mutant allele of *SCA1* in transgenic mice leads to disparate effects on motor behaviors followed by a progressive cerebellar dysfunction and histological alterations. J. Neurosci. 1997; 17:7385–7395. [PubMed: 9295384]

Crespo-Barreto JM, Fryer JD, Shaw CA, Orr HT, Zoghbi HY. Partial loss of ataxin-1 function contributes to transcriptional dysregulation in spinocerebellar ataxia type 1 pathogenesis. PLoS Genet. 2010; 6:e1001021. [PubMed: 20628574]

Dansithong W, Paul S, Figueroa KP, Rinehart MD, Wiest S, Pflieger LT, Scoles DR, Pulst SM. Ataxin-2 regulates RGS8 translation in a new BAC-SCA2 transgenic muse model. PLoS Genetics. 2015; 11:e1005182. [PubMed: 25902068]

de Chiara C, Giannini C, Adinoff S, de Boer J, Guida S, Ramos A, Jodice C, Kioussis D, Pastore A. The AXH module: an independently folded domain common to ataxin-1 and HBP1. FEBS Letter. 2003; 551:107–112.

de Chiara C, Menon RP, Strom M, Gibson TJ, Pastore A. Phosphorylation of S776 and 14-3-3 Binding Modulate Ataxin-1 Interaction with Splicing Factors. PLoS ONE. 2009; 4:e8372. [PubMed: 20037628]

Doyle JP, Dougherty JD, Heiman M, Schmidt EF, Stevens TR, Ma G, Bupp S, Shrestha P, Shah RD, Doughty ML, Gong S, Greengard P, Heintz N. Application of a translational profiling approach for the comparative analysis of CNS cell types. Cell. 2008; 135:749–762. [PubMed: 19013282]

Duarte-Neves J, Goncalves N, Cunha-Santos J, Simões AT, den Dunnen WFA, Hirai H, Kügler S, Cavadas C, de Almeida LP. Neuropeptide Y mitigates neuropathology and motor deficits in mouse models of Machado-Joseph disease. Hum. Mol. Genet. 2015; 24:5451–5463. [PubMed: 26220979]

Dufresne M, Seva C, Fourmy D. Cholecystokinin and gastrin receptors. Physiol. Rev. 2006; 86:805–847. [PubMed: 16816139]

Duvick L, Barnes J, Ebner B, Agrawal S, Andresen M, Lim J, Giesler GJ, Zoghbi HY, Orr HT. SCA1-like disease in mice expressing wild type ataxin-1 with a serine to aspartic acid replacement at residue 776. Neuron. 2010; 67:929–935. [PubMed: 20869591]

Emamian ES, Kaytor MD, Duvick LA, Zu T, Susan K, Tousey SK, Zoghbi HY, Clark HB, Orr HT. Serine 776 of ataxin-1 is critical for polyglutamine- induced disease in *SCA1* transgenic mice. Neuron. 2003; 38:375–387. [PubMed: 12741986]

Fogel BL, et al. Mutation of senataxin alters disease-specific transcriptional networks in patients with ataxia with oculomotor apraxia type 2. Hum. Mol. Genet. 2014; 2:4758–4769. [PubMed: 24760770]

Fryer JD, Yu P, Kang H, Mandel-Brehm C, Carter AN, Crespo-Barreto J, Gao Y, Flora A, Shaw C, Orr HT, Zoghbi HY. Exercise and genetic rescue of SCA1 via the transcriptional repressor Capicua. Science. 2011; 334:690–693. [PubMed: 22053053]

Gehrking KM, Andresen JM, Duvick L, Lough J, Zoghbi HY, Orr HT. Partial Loss of *Tip60* Slows Midstage Neurodegeneration in a Spinocerebellar Ataxia Type 1 (SCA1) Mouse Model. Hum. Mol. Genet. 2011; 20:2204–2212. [PubMed: 21427130]

Goff, L.; Trapnell, C.; Kelley, D. CummeRbund: Analysis, exploration, manipulation, and visualization of Cufflinks high-throughput sequencing data. R package version 2.8.22013. http://compbio.mit.edu/cummeRbund/

Huttlin EL, Jedrychowski MP, Elias JE, Goswami T, Rad R, Beausoleil SA, Vilén J, Haas W, Sowa ME, Gygi SP. A tissue-specific atlas of mouse protein phosphorylation and expression. Cell. 2010; 143:1174–1189. [PubMed: 21183079]

Jafar-Nejad P, Ward CS, Richman R, Orr HT, Zoghbi HY. Regional rescue of spinocerebellar ataxia type 1 phenotypes by 14-3-3E haploinsufficiencey in mice underscores complex pathogenicity in neurodegeneration. Prc. Natl. Acad. Scu USA. 2011; 108:2142–2147.

Jordan J, Greenway FL, Leiter LA, Li Z, Jacobson P, Murphy K, Hill J, Kler L, Aftring RP. Stimulation of cholecystokinin-A receptors with G181771X does not cause weight loss in overweight or obese patients. Clin. Pharm. & Thera. 83:281. (2118).

Jorgensen ND, Andresen JM, Lagalwar S, Armstrong B, Stevens S, Byam CE, Duvick LA, Lai S, Zoghbi HY, Clark HB, Orr HT. Phosphorylation of ATXN1 at Ser776 in the Cerebellum. J. Neurochem. 2009; 110:675–686. [PubMed: 19500214]

Kawamura-Saito M, Yamazaki Y, Kaneko K, Kawaguchi N, Kanda H, Mukai H, Gotoh T, Motoi T, Fukayama M, Aburatani H, Takizawa T, Nakamura T. Fusion between CIC and DUX4 up-regulates PEA3 family genes in Ewing-like sarcomas with t(4;19)(q35;q13) translocation. Hum. Mol. Genet. 2006; 15:2125–2137. [PubMed: 16717057]

Kim E, Lu H-C, Zoghbi HY, Song J-J. Structural basis of protein complex formation and reconfiguration by polyglutamine disease protein Ataxin-1 and Capicua. Genes Dev. 2013a; 27:590–595. [PubMed: 23512657]

Kim D, Pertea G, Trapnell C, Pimentel H, Kelley R, Salzberg SL. TopHat2: accurate alignment of transcriptomes in the presence of insertions, deletions and gene fusions. Genome Biology. 2013b; 14:R36. [PubMed: 23618408]

Klement IA, Skinner PJ, Kaytor MD, Yi H, Hersch SM, Clark HB, Zoghbi HY, Orr HT. Ataxin-1 nuclear localization and aggregation: Role in polyglutamine-induced disease in *SCA1* transgenic mice. Cell. 1998; 95:41–53. [PubMed: 9778246]

Klockgether T. Update on degenernative ataxias. Curr. Opin. Neurol. 2011; 24:339–345. [PubMed: 21734495]

Koeppen AH. The pathogenesis of spinocerebellar ataxia. Cerebellum. 2005; 4:62–73. [PubMed: 15895563]

Lam, Y.C, Bowman, A.B.; Jafar-Nejad, P.; Lim, J.; Richman, R.; Fryer, JD.; Hyun, E.; Duvick, L.A, Orr, H.T.; Botas, J.; Zoghbi, HY. Mutant ATAXIN-1 interacts with the repressor Capicua in its native complex to cause SCA1 neuropathology. Cell. 2006; 127:1335–1347. [PubMed: 17190598]

Langfelder P, Horvath S. WGCNA: an R package for weighted correlation network analysis. BMC Bioinformatics. 2008; 2008:9–559.

Langfelder P, Mischel PS, Horvath S. When is hub gene selection better than standard meta-analysis? PLoS ONE. 2013; 8:e61505. [PubMed: 23613865]

Lay JM, Gillespie PJ, Samuelson LC. Murine prenatal expression of cholecystokinin in neural crest, enteric neurons, and enteroendocrine cells. Develop. Dynamics. 1999; 216:190–200.

Lee SY, Soltesz I. Cholecystokinin: a multi-functional molecular switch of neuronal circuits. Dev. Neurobiol. 2011; 71:83–91. [PubMed: 21154912]

Len ES, et al. Genome-wide atlas of gene expression in the adult mouse brain. Nature. 2007; 445:168–176. [PubMed: 17151600]

Lidwell K, Griffiths R. Possible role for the FosB/JunD AP-1 transcription factor complex in glutamate-mediated excitotoxicity in cultured cerebellar granule cells. J. Neurosci. Res. 2000; 62:427–439. [PubMed: 11054812]

Lim J, Crespo-Barreto J, Jafar-Nejad P, Bowman AB, Richman R, Hill DE, Orr HT, Zoghbi HY. Opposing effects of polyglutamine expansion on native protein complexes contribute to SCA1. Nature. 2008; 452:713–719. [PubMed: 18337722]

Lin X, Antalffy B, Kang D, Orr HT, Zoghbi HY. Polyglutamine expansion downregulates specific neuronal genes before pathologic changes in SCA1. Nat. Neurosci. 2000; 3:157–163. [PubMed: 10649571]

Liu C, Lin C, Whitaker D.T, Bakeri, H. Bulgakov OV, Liu P, Lei J, Dong L, Li T, Swaroop A. Prickel1 is expressed in distinct cell populations of the central nervous system and contributes to neuronal morphogenesis. Hum. Mol. Genet. 2013; 22:2234–2246. [PubMed: 23420014]

Machanick P, Bailey TL. MEME-ChIP motif analysis of large DNA datasets. Bioinfomatics. 2011; 27:1696–1697.

Matilla A, Roberson ED, Banfi S, Morales J, Armstrong DL, Burright EN, Orr HT, Sweatt JD, Zoghbi HY, Matzuk MM. Mice lacking Ataxin-1 display learning deficits and decreased hippocampal paired-pulse facilitation. J. Neurosic. 1998; 18:5508–5516.

Oldham MC, Konopka G, Iwamoto K, Langfelder P, Kato T, Horvath S, Geschwind DH. Functional organization of the transcriptome in human brain. Nat. Neurosci. 2008; 11:1271–1282. [PubMed: 18849986]

Orr HT, Chung MY, Banfi S, Kwiatkowski TJ Jr. Servadio A, Beaudet AL, McCall AE, Duvick LA, Ranum LP, Zoghbi HY. Expansion of an unstable trinucleotide CAG repeat in spinocerebellar ataxia type 1. Nat. Genet. 1993; 4:221–226. [PubMed: 8358429]

Parikshak NN, Gandal MJ, Geschwind DH. Systems biology and gene networks in neurodevelopmental and neurodegenerative disorders. Nat. Rev Genet. 2015; 16:441–458. [PubMed: 26149713]

Prudencio M, et al. Distinct brain transcriptome profiles in C9orf72-associated and sporadic ALS. Nat. Neurosci. 2015; 18:1175–1182. [PubMed: 26192745]

Roberts A, Trapnell C, Donaghey J, Rinn JL, Pachter L. Improving RNA-Seq expression estimates by correcting for fragment bias. Genome Biology. 2011; 12:R22. [PubMed: 21410973]

Rong Y, Wang T, Morgan JL. Identification of candidate Purkinje cellspecific markers by gene expression profiling in wild-type and *pcd*^{2J} mice. Mol. Brain Res. 2004; 132:128–145. [PubMed: 15582153]

Ruegsegger C, Stucki DM, Steiner S, Angliker N, Radecke J, Keller E, Zuber B, Rüegg MA, Saxena S. Impaired mTORC1-dependent expression of Homer-3 influences SCA1 pathophysiology. Neuron. 2016; 89:129–146. [PubMed: 26748090]

Schorge S, van de Leemput J, Singleton A, Houlden H, Hardy J. Human ataxias: a genetic dissection of inositol triphosphate receptor (ITPR1)-dependent signaling. Trends Neurosci. 2010; 33:211–219. [PubMed: 20226542]

Serra HG, Byam CE, Lande JD, Tousey SK, Zoghbi HY, Orr HT. Gene profiling links SCA1 pathophysiology to glutamate signaling in Purkinje cells of transgenic mice. Hum. Mol. Genet. 2004; 13:2535–2543. [PubMed: 15317756]

Serra HG, Duvick L, Zu T, Carlson K, Stevens S, Jorgensen N, Lysholm A, Burright E, Zoghbi HY, Clark HB, Andresen JM, Orr HT. RORa-mediated Purkinje cell development determines disease severity in adult *SCA1* mice. Cell. 2006; 127:697–708. [PubMed: 17110330]

Tissir F, Goffinet AM. Shaping the nervous system: role of the core planar cell polarity genes. Nat. Rev. Neurosci. 2013; 14:525–535. [PubMed: 23839596]

Trapnell C, Williams BA, Pertea G, Mortazavi A, Kwan G, van Baren MJ, Salzberg SL, Wold BJ, Pachter L. Transcript assembly and quantification by RNA-Seq reveals unannotated transcripts and isoform switching during cell differentiation. Nat. Biotechnol. 2010; 28:511–515. [PubMed: 20436464]

Trapnell C, Roberts A, Goff L, Pertea G, Kim D, Kelley DR, Pimentel H, Salzberg SL, Rinn JL, Pachter L. Differential gene and transcript expression analysis of RNA-seq experiments with TopHat and Cufflinks. Nat Protoc. 2012; 7:562–578. [PubMed: 22383036]

Tsai C-C, Kao H-Y, Mitzutani A, Banayo E, Rajan H, McKeown M, Evans RM. Ataxin 1, a SCA1 neurodegenerative disorder protein, is functionally linked to the silencing mediator of retinoid and thyroid hormone receptors. Proc. Natl. Acad. Sci. U. S. A. 2004; 101:4047–4052. [PubMed: 15016912]

Tsuda H, Jafar-Nejad H, Patel AJ, Sun Y, Chen H-K, Rose MF, Venken KJT, Botas J, Orr HT, Bellen HJ, Zoghbi HY. The AXH domain in mammalian/*Drosophila* Ataxin-1 mediates neurodegeneration in spinocerebellar ataxia 1 through its interaction with Gfi-1/Senseless proteins. Cell. 2005; 122:633–644. [PubMed: 16122429]

Vandaele S, Nordquist DT, Feddersen RM, Tretjakoff I, Peterson AC, Orr HT. Purkinje-cell-protein-2 regulatory regions and transgene expression in cerebellar compartments. Genes Develop. 1991; 5:1136–1148. [PubMed: 2065970]

Wang L, Hubert JA, Lee SJ, Pan J, Qian S, Reitmen ML, Strack AM, Weingarth DT, MacNeil DJ, Weber AE, Edmondson SD. Discovery of pyrimidine carboxamides as potent and selective CCK1 reeptor agonists. Bioor. Med. Chem. Letts. 2011; 21:2911–2915.

Yue S, Serra HG, Zogbhi HY, Orr HT. The spinocerebellar ataxia type 1 protein, ataxin-1, has RNA-binding activity that is inversely affected by the length of its polyglutamine tract. Hum. Mol. Genet. 2001; 10:25–30. [PubMed: 11136710]

Zhang B, Horvath S. A general framework for weighted gene co-expression network analysis. Stat. Appl. Genet. Mol. Biol. 2005; 4 article 17.

Highlights

- Analysis of RNA-seq from SCA1 mice reveals two modules that correlate with disease
- ATXN1- Cic interaction is a driver of expression change that correlate with disease
- *Cck* upregulation and interaction with Cck1R protect PCs from progressive pathology

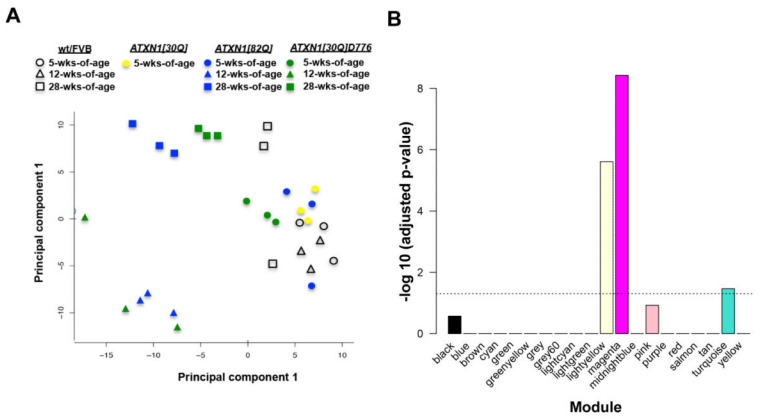

Figure 1. Network analysis of *ATXN1* mouse cerebellar gene expression

(A) Principal component analysis of *ATXN1* transgenic mouse cerebellar RNA-seq data. (B) Correlation with disease for weighted gene co-expression analysis (WGCNA) Modules. Colors of bars correspond to WGCNA Module. Dashed line depicts statistical significance.

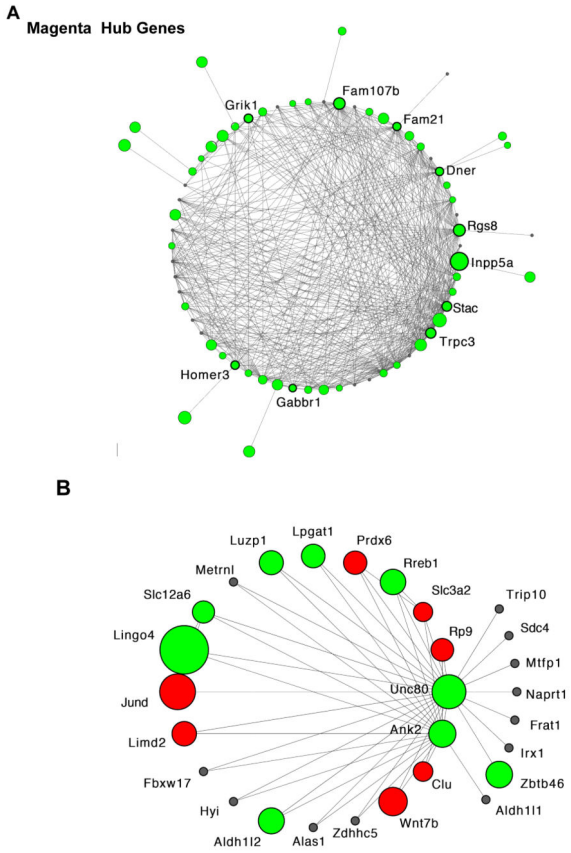

Figure 2. WGCNA Modules Significantly Associated with Ataxia in ATXN1 Mice

For clarity only the most highly connected members of each module are depicted. Size of the circles is scaled by the absolute value of the mean log2 fold change between *ATXN1[82Q]* and wt/FVB, and between *ATXN1[30Q]D776* and wt/FVB. (A) The Magenta network. Green are genes significantly down-regulated *ATXN1[82Q]* and *ATXN1[30Q]D776* vs wt/FVB cerebella. The top 10 Magenta hub genes (Table S4), those with the highest intramodular connectivity, are in bold. (B) The Lt Yellow network Hub genes. Grey indicts genes whose expression either did differ significantly from wt/FVB or differed in opposite directions in *ATXN1[82Q]* and *ATXN1[30Q]D776* vs wt/FVB cerebella.

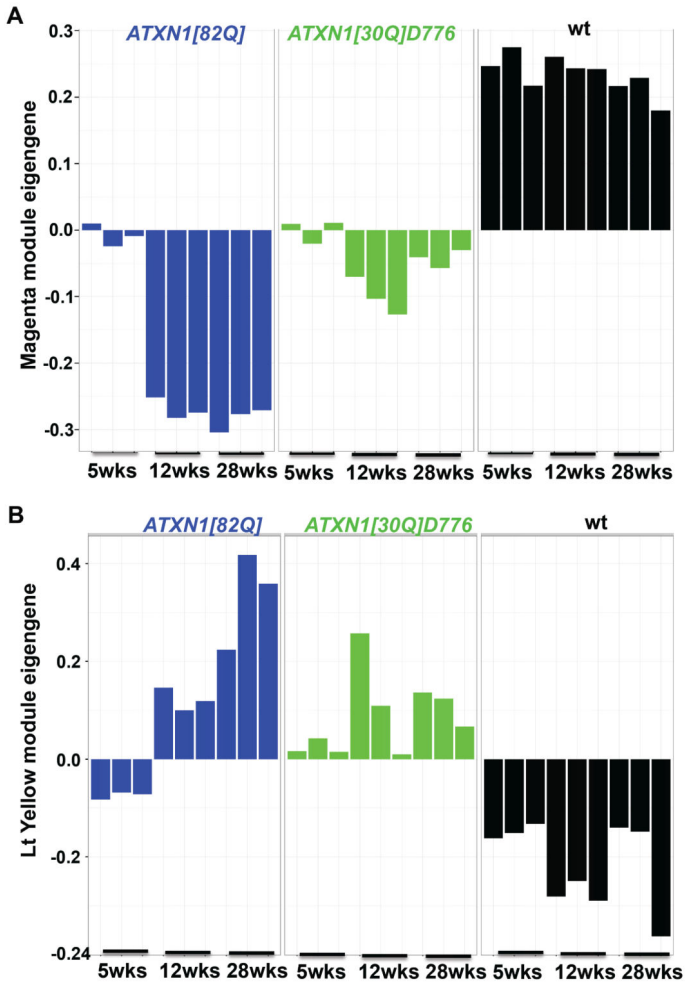

Figure 3.

(A) Magenta Module eigengene changes in *ATXN1[82Q]*, *ATXN1[30Q[D776*, and wt (FVB/NJ) with increasing age, 5, 12 , and 28 weeks. (B) Lt Yellow Module eigengene changes in *ATXN1[82Q]*, *ATXN1[30Q[D776*, and wt with increasing age, 5, 12 , and 28 weeks. See Tables S2 and S3.

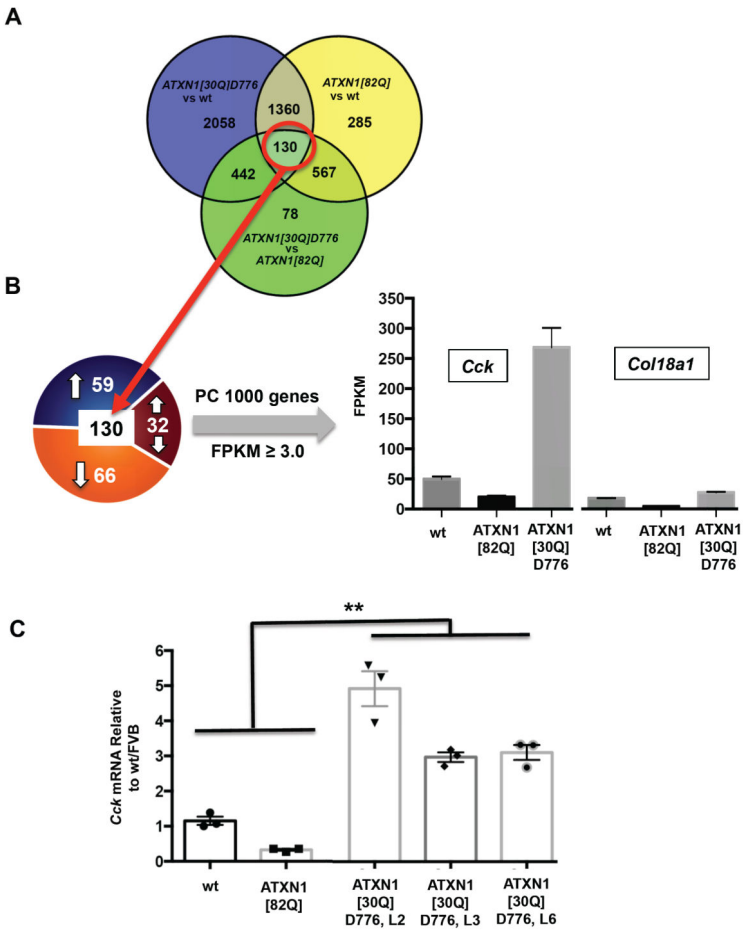

Figure 4. Expression of cholecystokinin (*Cck*) is elevated in *ATXN1[30Q]D776* cerebella

(A) Venn diagram depicting the total number of transcripts changed at 12 weeks of age. (B) Breakdown of the expression changes for the 130 genes with significant changes in common between *ATXN1[82Q]* and *ATXN1[30Q]D776* cerebella. Fifty-nine genes were upregulated in both compared to wt (FVB/NJ) and 66 genes downregulated. Thirty-two genes changed in opposite directions in *ATXN1[82Q]* and *ATXN1[30Q]D776* cerebella. Of these 32 genes, two genes (*Cck* and *Col18a1*) had expression levels of FPKM ≥ 3.0 and enhanced translation in Purkinje cells. (C) qRT PCR validation of elevated *Cck* cerebellar expression in *ATXN1[30Q]D776* mice relative to other *ATXN1* transgenic lines.

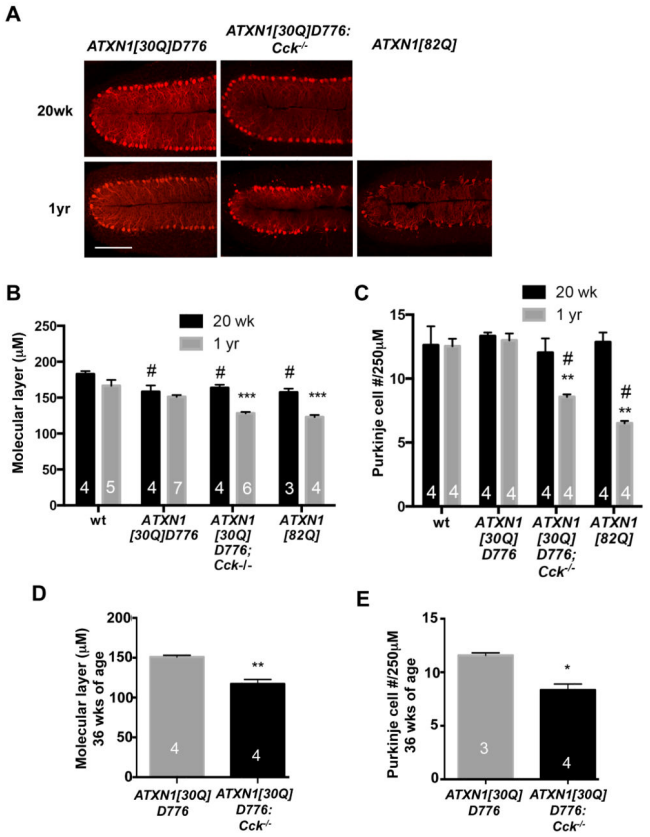

Figure 5. Elevated *Cck* expression is protective against progressive Purkinje cell atrophy and death in *ATXN1[30Q]D776* mice

(A) Representative images depicting primary cerebellar fissure showing PC morphology revealed by calbindin immunostaining. Scale bar, 200 µM applies to all images in this panel. (B) Changes in cerebellar molecular layer thickness for examined genotypes at 20 weeks of age vs 1 year of age. (C) PC counts for examined genotypes at 20 weeks of age vs 1 year of age. Calbindin-positive PC bodies were counted within the primary fissure per 250µM. Data in (B) and (C) are represented as mean, ±SEM. Two-Way ANOVA, Tukey post-hoc test. # indicates $p<0.01$ compared to wt. *$p<0.05$, **$p<0.01$, and ***$p<0.001$ comparing 1 year to 20 wks. Numbers of cerebella analyzed per genotype and age are indicated within each bar. (D) Changes in cerebellar molecular layer thickness at 36 weeks of age in *ATXN1[30Q]D776* and *ATXN1[30Q]D776*: $Cck^{-/-}$ mice. ± SEM, Student's t-test. **$p<0.002$. (E) Purkinje cell counts for per 250µM at 36 weeks of age in *ATXN1[30Q]D776* and *ATXN1[30Q]D776*: $Cck^{-/-}$ mice. Data mean, ± SEM. Student's t- test. *$p<0.01$.

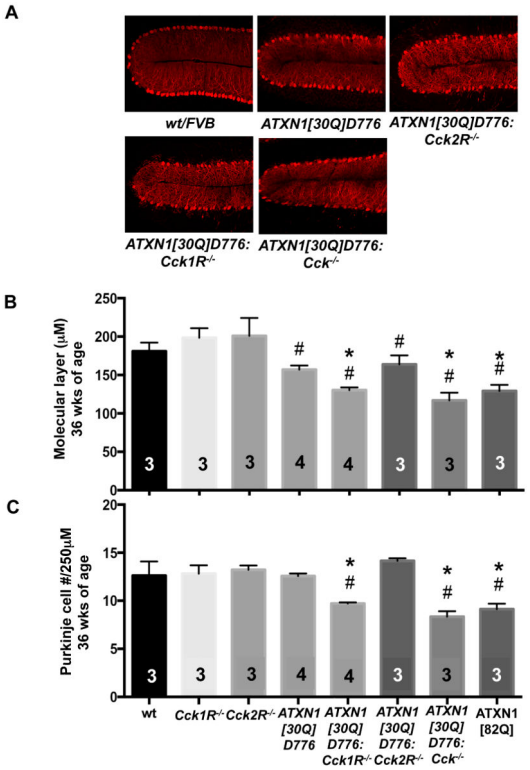

Figure 6. *Cck1R* is required for protection against progressive Purkinje cell atrophy and death in *ATXN1[30Q]D776* mice

(A) Representative images depicting primary cerebellar fissure showing PC morphology revealed by calbindin immunostaining. (B) Cerebellar molecular layer thickness for examined genotypes at 36 weeks of age. (C) PC counts for examined genotypes at 36 weeks of age. Calbindin- positive PC bodies were counted within the primary fissure per 250μM. Data in (B) and (C) mean, ±SEM. Two-Way ANOVA, Tukey post-hoc test. # indicates $p<0.002$ compared to wt. *$p<0.01$ compared to *ATXN1[30Q]D776*.

Table 1

Expression of ATXN1 Cerebellar WGCNA Module Genes

				ISH Pattern (Allen Brain Atlas)		
Module (adjusted p-value)	**Genes**	**Overlap-M6D PC Network***	**PC-enriched Translation****	**I PC-exclusive**	**II Multiple Cell Types**	**I/II**
Magenta	342	19	94 (27%)	175 (51%)	31 (9%)	5.6
Lt Yellow	35	9	1 (3%)	11 (31%)	8 (22%)	1.4

* Oldahm et al. (2008)

** Doyle et al. (2008)

Table 2

Presence of Cic-bindng Motifs in Magenta and Lt Yellow Module

Cic Binding Motif	**Module**		
TGAATGAA	**Magenta**	**Control***	**p value**
Genes motif present	149	61	2.73e-12
Genes motif not present	190	278	
TGAATGGA	**Magenta**		
Genes motif present	180	100	5.85e-10
Genes motif not present	159	239	
TGAATGAA	**Lt Yellow**		
Genes motif present	5	6	ns
Genes motif not present	29	28	
GAATGGA	**Lt Yellow**		
Genes motif present	18	7	0.005
Genes motif not present	14	27	

The promoter sequences (2kb upstream of TSS) of each gene in the two modules were extracted from human reference hg19 genome. Sequence Fasta files were used as input to theFIMO software (http://meme-suite.org/tools/fimo) to scan sequence database for matches to each motif. Occurrence of the two Cic motifs in promoter sequence and control sequence

*(Randomized sequence for each gene in module) were counted. Fisher's extact test was used to measure the enrichment significance of the two motifs in Magenta and Light yellow modules.